ns-3 Simulation Based Exploration of LTE Handover Optimization

Sachin Nayak*

University of Washington, Seattle, USA

Abstract

Network simulator (ns-3) is a reputed simulation platform for performance evaluation of cellular networks. In this work, we explore the use of ns-3 for tracking of successful handovers (HO) and handover failures and consequent impact on 4G LTE network throughput with the aim of discovering new analytical relations about HOs and new methods to optimize the resulting throughput. Decreased cell sizes in newer generation networks lead to increasing number of handovers and handover failures that have significant impact. We begin by reviewing analytical models in the literature that aim to predict number of HO and HO failures in terms of HO control and network parameters. We initially conduct a suite of exhaustive validation studies of such analytical models, based on the simulation execution manager (SEM) for ns-3 for parallelization. Via this, we discover new causal relations relating HO failures and choice of HO control parameters on network throughput. Based on these initial results, we next evaluate the application of Gaussian process regression for prediction of instantaneous network throughput and bandit algorithms as an effective mechanism to optimize throughput over time. The new relations discovered help better understand the impact of input handover control parameters on the number of handovers and handover failures allowing us to fine tune them. The new optimization and prediction methods discovered give good gains over baseline algorithms and help accurately predict throughput respectively.

1. Introduction

Network densification is a key feature of cellular network evolution; as 5G aims to achieve peak data rate of Gbps [1] to users. The use of higher frequency bands (mmWave) and large channelization bandwidths along with large-scale MIMO, naturally also lead to such network densification as means to increase network capacity via smaller cell sizes and greater frequency reuse.

A direct consequence of shrinking cell sizes is the expected increase to rate of handovers (HOs) that impose significant overhead in terms of mobility management and HO monitoring and optimization. Further, deployment of heterogeneous networks overlays - small cells and macro cells - contribute to even more HOs and increased radio link failure (RLF) rates, respectively. Hence, mobile network operators (MNOs) require accurate and real-time visibility of the network variables such as number of HOs and RLFs to provide appropriate quality of service to end users (e.g., guaranteed data rates and upper bound on radio link failures). HO is the process of transferring an associated user entity (UE) from a current serving cell base station (BS) to a future target cell BS while RLF occurs due to loss of connection between UE to a (current) cell BS resulting from link conditions.

A successful handover in LTE consists of a set of events occurring according to the 3GPP protocol as shown in Fig. 1. The UE is configured to send measurement reports of received power for the source BS or eNodeB (eNB) and neighboring eNBs. Based on the reports received, the source eNB takes a decision to perform HO based on a HO algorithm and performs

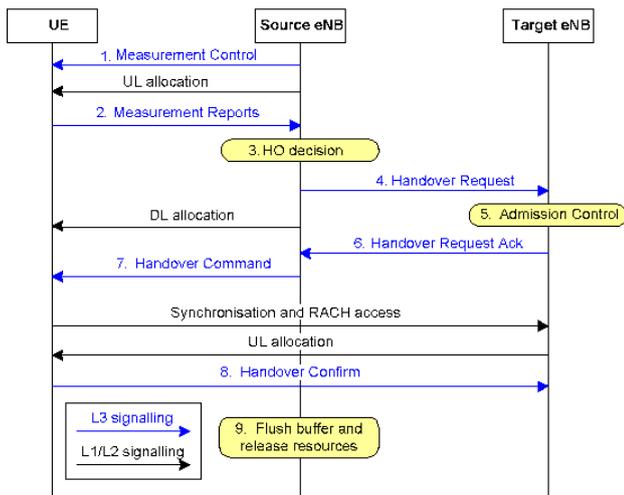*Corresponding author. Email: sachinn@uw.edu

Figure 1. Successful Handover Procedure in LTE [2]

procedures for admission control with the target eNB. This leads to a handover command being sent to the UE followed by synchronization and Random Access Channel (RACH) procedure finally leading to the reception of HO confirmation at the target eNB. If the parameters of the HO algorithm are improperly configured, a HO failure happens. HO failure means that no HO occurs, HO procedure is not completed or HO occurs too early. A HO failure is accompanied by an RLF due to weak signal strength as a result of improper BS assignment. In the dense scenarios that we consider in this paper, HO failures and RLFs are equivalent as the probability of the occurrence of handover failure as no handover with no RLF or HO failure due to lost control packets is very low.

1.1. Motivation

Both HOs and RLF cause decrease in throughput but the impact of RLFs tend to be costlier as the recovery is more time consuming[1]. However, the relationship between the input parameters and the output variables of number of HOs, number of HO failures and the throughput is complex. This needs a network simulator like ns-3 for requisite exploration. While analytical models do exist [3] [4], they have been defined for specific scenarios that may not be applicable to a typical scenario in ns-3 or the real-world. Since the number of RLFs and HOs that occur are coupled, it is difficult to minimize both simultaneously. This necessitates a need for simulation study building upon

---

[1]Nonetheless, a small number of HOs is necessary as it can prevent RLFs and UEs from holding on to weaker cells draining battery and lower data rates due to selection of low modulation and coding schemes.

prior theoretical literature. Moreover, prediction (and thus optimization) of network throughput at a given set of network parameters and time instant is not possible, requiring simulation-based algorithms from machine learning and optimization to achieve the best data rates.

As network operations will small cells become more complex and challenging to manage and optimize, operators are increasingly exploring new techniques to manage HOs and RLFs to minimize their impact on the network. Network equipment vendors have proposed new approaches such as conditional HO [5] [6] enlisting multiple target cells and reducing HO interruption times [7]. More handover algorithms, e.g., heuristic and artificial intelligence-based solutions, especially emerging graph-based deep learning models [8] [9] [10] [11] are being suggested. Optimizing HO parameters for attaining improved system performance - while considering joint optimization of throughput, number of HOs and RLFs is thus becoming increasingly important in next-G networks.

Our study explores understanding of the elements of the existing protocol pertaining to HO based on analytical relations. It also aims to maximize throughput under the impact of HOs and RLFs by optimizing the HO control parameters. We quantify relationships between the input parameters to HOs in LTE network and the output variables as shown in Fig.2 as well as optimization algorithms for network throughput, using the well-respect network simulation framework ns-3. The large number of input parameter combinations and output variables necessitates a simulation platform to achieve these objectives.

The ns-3 LENA [12] LTE module supports study of network handover [13], however any detailed validation study of HO is yet to be documented. To reduce runtimes, it is desired to use parallel simulations via the simulation execution manager (SEM) [14]. The relations that were validated, and the algorithms devised provide a good foundation for prediction and optimization of performance in real world networks. Using them, network providers can arrive at a healthy compromise between the number of HOs and RLFs to achieve the best throughputs based on their heuristic policies.

1.2. Previous Work on LTE Network Analysis Under HOs

The default HO algorithm in ns-3 is the A3 reference signal received power (RSRP) HO algorithm [15], described in detail in Section II.A, that has the three inputs of `hysteresis`, `timeToTrigger` and `a3Offset` as shown in Fig. 2. Existing HO models in the literature are mainly based on stochastic geometry [3] [4] [16]. They model HO and HO failure locations using concentric circles and estimate the respective probability density functions by modeling
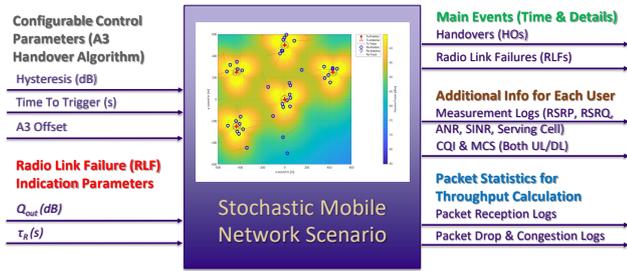
Figure 2. Inputs parameters and output variables of mobile network scenario; RSRQ – Reference Signal Received Quality, ANR– Automatic Neighbour Relation, CQI– Channel Quality Index, MCS– Modulation and Coding Scheme

user positions as Poisson Point Processes with linear trajectories. Closed-form expressions for the HO and HO failure probability are obtained in terms of the user speed and the `timeToTrigger` for the additive noise channel. Extensions to include channel models with fading and shadowing were considered in [17]; however, this does not include the parameters of `hysteresis` and `a3offset`.

The impact of the HO control parameters like `hysteresis` and `timeToTrigger` on network throughput and its prediction & optimization in terms of them is never studied. System level evaluation of throughput in 3GPP reference scenarios [18] or performance evaluation study of simple handover metrics and throughput [19] [20] have been performed, but no direct relation between throughput and the HO control parameters has been discovered. This provides ample scope for applying tools from machine learning and optimization like Gaussian process regression and bandit algorithms for the purpose of throughput prediction and optimization. Moreover, prior studies do not consider non-standard values of handover control parameters and their optimization over time.

In addition, there exist some other industry-based simulation studies [21] [22] [23] that optimize the HO control parameters for specific scenarios, providing additional hints for run-time tuning. These include finer classifications of HOs and RLF events such as i) too-early RLFs, ii) too-late RLFs and iii) ping-pong HOs that cannot be measured within ns-3 simulation runs that only allow estimation of the number of HOs and RLFs. The relevant expressions from the literature are described in Section II.B.

1.3. Contributions

The main contributions of this paper are threefold of HOs, HO failures and throughput in LTE networks. This was achieved through a careful study using a simulation platform based on the ns-3 LENA module and SEM.

1. Validation of the analytical relations pertaining to HOs and RLFs in the literature to produce additional (statistically justified) insights into causal (between parameter inputs and measured outputs) relations based on inferences from simulation traces.

2. Discovery of the three additional relations never discussed in the literature:

   (a) #HOs $\propto$ speed/timeToTrigger
   (b) #RLFs $\propto$ speed $*$ hysteresis
   (c) #HOs $\propto$ speed/hysteresis.

   This helps us form a deeper understanding of HOs and their control parameters.

3. Application of Gaussian process regression and bandit algorithms for the purpose of network throughput prediction and optimization in terms of HO control parameters, as HOs and RLFs affect network throughput.

1.4. Organization

Section II contains a short technical description of relevant parts of the long term evolution (LTE) standard, system setup, interface used and known HO relations from literature. Following this, simulation results obtained by our platform for validating HO relations and discovering new ones along with the runtime details are provided in Section III. Section IV is dedicated to the impact of the HOs and RLFs on throughput, its prediction and optimization in terms of HO control parameters. Finally, Section V concludes with a brief discussion of the results.

2. System Setup and Known Relations

We next provide a short overview of the A3 HO algorithm and RLF detection as per the LTE standard, followed by a description of the system setup and interface of the simulation platform based on ns-3 + SEM.

2.1. A3 Handover Algorithm

The A3 RSRP HO algorithm is illustrated in Fig. 3. The physical significance of the A3 HO algorithm is that it tries to assign the cell with the strongest signal to the UE. Hence, it is also called the strongest cell algorithm. Consider a user entity (UE) moving away from its serving cell towards a neighbor cell (or target cell). The reference signal receiver power (RSRP) from both the cells is measured at the UE and reported back
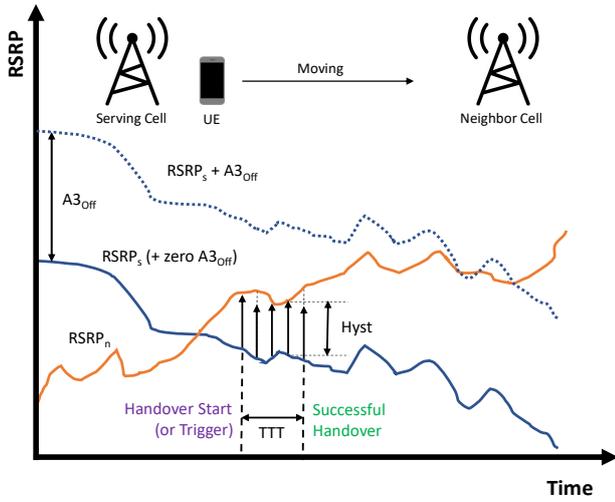
Figure 3. A3 HO Algorithm

to base stations (eNB) through measurement reports [2]. The A3 event is defined as the event where the neighbor cell signal strength is greater than the serving cell signal strength by an offset. The condition for a successful handover is given below [24].

$$RSRP_n > RSRP_s + A3_{Off} + Hyst \text{ for } TTT \quad (1)$$

where

$RSRP_n(dB)$- RSRP of neighbor cell (or target cell)

$RSRP_s(dB)$- RSRP of serving cell (or source cell)

$A3_{Off}(dB)$- a3offset is the offset by which the difference in RSRPs is shifted

$Hyst(dB)$- hysteresis is the HO margin above which the RSRP difference must stay put for successful HO

$TTT(s)$- timeToTrigger is the time for which HO margin must be met for successful HO

In other words, successful handover occurs when the difference between the RSRP of target cell and source cell offset by a3offset is greater than hysteresis for a time duration of timeToTrigger. Handover does not occur if the difference between the two RSRPs along with the offset becomes less than the hysteresis value even for an instant during the handover or if equation (1) is never met. Fig. 3 shows the case of a successful handover where the RSRP of the neighbor cell (orange) is greater than the RSRP of the serving cell (blue) by the hysteresis triggering the start of a handover and stays equal to or above the required margin until completion

---

[2]RSRP is measured based on pilot symbols from decoded reference signals.

Table 1. Standard values for configurable HO parameters [24]

Parameter	Values
hysteresis (dB)	0, 0.5, ... 2, ... 14.5, 15
timeToTrigger (ms)	0, 40, 64, 100, 128, 160, 256, 320, 480, 512, 640, 1024, 1280, 2560, 5120
a3offset (dB)	-15, -14.5, ... 0, ... 14.5, 15

of the handover procedure. The dotted line represents the case when the a3offset is set to a wrong non-zero value from the default value of zero, leading to no handover as the A3 HO condition is never met although the current scenario necessitates a handover to support UE connectivity. The role of offset in the A3 handover algorithm is to make the serving cell look better than its current measurement in comparison to the neighbor and can be used to prevent unnecessary handovers. Handover causes temporary interruption of data flow due to loss of connection. The time measured from the handover trigger to the successful completion including the radio resource control (RRC) procedures is called the handover interruption time (HIT).

The standard values for the configurable handover parameters are shown in Table 1 [24]. Exploration of the parameter space via ns-3 simulation is an active research direction for understanding HO and RLF modeling, and its impact on network throughput, with the caveat that the full range of values may not be available in deployed networks due to operational hardware constraints.

2.2. Radio Link Failure (RLF) Detection

A contributing factor to handover failure are RLFs, representing loss of the UE-to-eNB link, mainly due to degradation caused by channel conditions, as illustrated in Fig. 4. Such link loss is caused by packet decoding failure, resulting for example due to the presence of additional interference from neighbour cells as well degradation of received signal power from the source cell. Hence, the Signal-to-Interference+noise-Ratio (SINR) as measured at the UE input is given by Equation (2).

$$SINR = \frac{RSRP_s}{RSRP_n + \sigma^2} \quad (2)$$

where $RSRP_s$ and $RSRP_n$ are the RSRPs of the serving and neighbor cell respectively and σ^2 is the noise power as measured at the UE. RLF occurs when the SINR falls below a threshold continuously for a specified duration, i.e.,

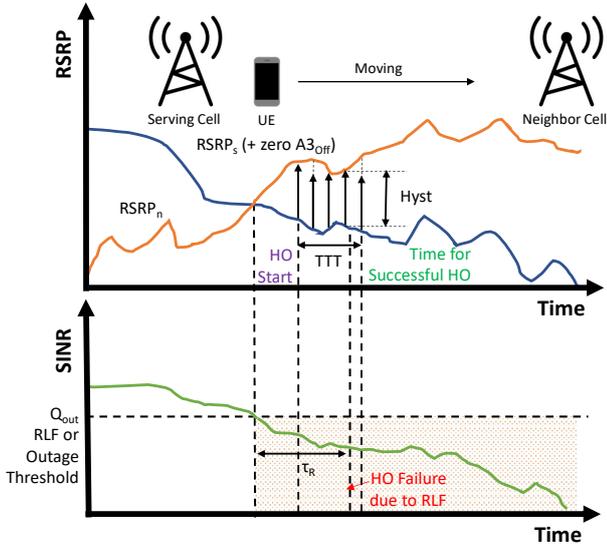$$SINR < Q_{out} \text{ for } \tau_R \quad (3)$$

Figure 4. RLF detection

where $Q_{out}(dB)$ is the outage threshold for RLF and $\tau_R(s)$ is the outage duration. The default value of $Q_{out}(dB)$ is -5dB in ns-3 and $\tau_R(s)$ tends to be around 100 ms based on the RRC procedures used [25].

This kind of failure is called too-late HO failure or too-late RLF, as the RLF occurs before the time instant for successful HO, i.e., the HO process is triggered too late. RLFs can also occur just after successful handover, labeled as too-early handover since the HO process is triggered too early, or otherwise when there are no links available for HO in the target cell. In ns-3, it is hard to classify RLFs as i) too-late, ii) too-early or iii) otherwise. Most (>90%) of the RLFs in our study, due to the scenario with closely spaced cells, are too-late RLFs. In summary, RLFs are undesirable events in an LTE network and operators wish to minimize their occurrence by setting HO parameters correctly.

2.3. System Setup

In this work, we use the default `lena-dual-stripe` scenario as defined in the 3GPP standardization process [26]. This is a general scenario representative of a typical mobile network in a city. This scenario was chosen for its general nature with results applicable to any other scenario and because it appears in the standardization documents. We made modifications to ns-3 to include the functionality and input for the `a30ffset` parameter that is not present by default, and included additional input parameters like `hysteresis` and `timeToTrigger`. The parameters used for the simulation are described in Table 2 and the interface between SEM and ns-3 shown in Fig. 5. This platform
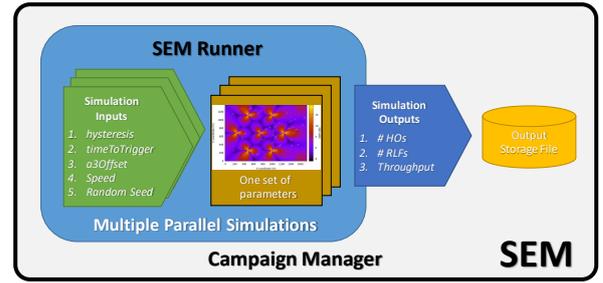

Figure 5. Interface between SEM and ns–3

Table 2. Parameter set used for the `lena-dual-stripe` scenario in ns–3 for simulation with SEM

Parameter	Description
Mobility	`SteadyStateRandomWaypointMobilityModel` (default) with min and max speed both set to `vel` input from SEM; changing mobility model keeping speed the same gives similar results
Buildings	No buildings are placed in the scenario by setting `nBlocks` to zero
Channel Model	`HybridBuildingsPropagationModel` used; default values used for the eNB (eNodeB or base station) TX power, bandwidth and EARFCN; no shadowing component is present as no buildings are placed
Simulation Time	`simTime` set to nominal 5s to obtain statistically significant results in reasonable time
Number of UEs	`macroUeDensity` set to `0.0002` to spawn around 50 UEs at random locations within the scenario bounding box based on `RngRun` and `RngSeed`
Network	EPC in both UL/DL with X2 interface added to enable HOs; UDP used to stream NGBR video to each UE over a single bearer
HO Control Parameters	Added code and additional input for `a30ffset`; `hysteresis`, `timeToTrigger` and `a30ffset` input by SEM; default RLF parameters used
Stochasticity	Fading, shadowing & UE mobility are stochastic elements with different values of `RngRun` and `RngSeed`

can be used to run multiple parallel simulations in ns-3 with different input configurations, leading to parsed output data frames in Python.

2.4. Impact of HO parameters

In this section, we discuss several relations between HO input parameters and HOs & HO failures, obtained by studying the A3 HO algorithm in Section IIA in the light of prior studies [22], [21], [23]. Although previous work does not explicitly state these relations, they can be obtained by surveying simulation data. These provide a good starting point for the HO and RLF validation process in ns-3 as well as for discovering
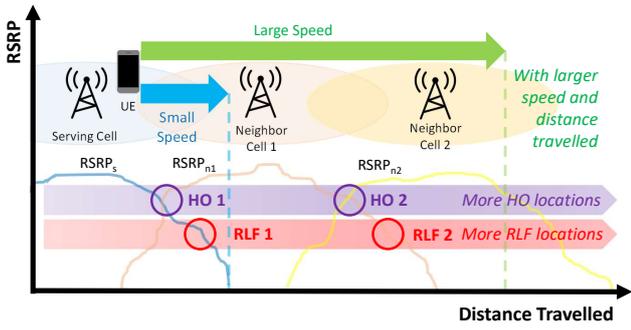
Figure 6. Effect of changing UE speed on the number of HOs and RLFs; simple illustration with three cells and one UE
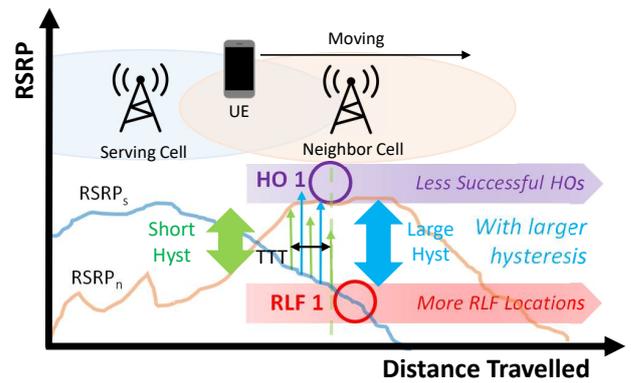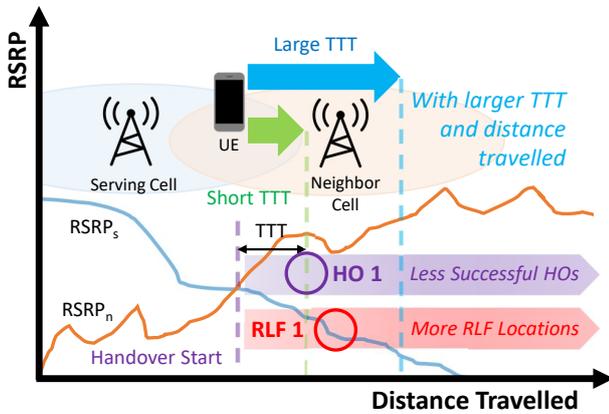

Figure 7. Effect of changing timeToTrigger on the number of HOs and RLFs; simple illustration with two cells and one UE

new relations.

Effect of UE Speed.

$$As \ \text{speed} \Uparrow, \#HOs \Uparrow \ and \ \#RLFs \Uparrow . \quad (4)$$

With higher speed, the UE moves past more cells per unit time, hence leading to larger number of HO opportunities. Simultaneously, it also leads to increased possibility of RLFs, due to SINR degradation as the RSRP of source cell degrades with distance and the interference due to the RSRP of neighbor cell increases. Fig. 6 illustrates this for a simple example of a single UE moving past three cells.

Effect of Changing timeToTrigger.

$$As \ \text{timeToTrigger} \Uparrow, \#HOs \Downarrow \ but \ \#RLFs \Uparrow . \quad (5)$$

Fig. 7 illustrates the effect of increasing timeToTrigger with the simple example of a single

Figure 8. Effect of changing hysteresis on the number of HOs and RLFs; simple illustration with two cells and one UE

UE moving past two cells. With the increase of timeToTrigger, the UE can move farther away from the serving cell before a HO is successfully completed, leading to lesser number of HOs. At the same time, as the UE moves away from the serving cell, an RLF can be readily caused due to the degraded RSRP and thus SINR implying that the number of RLFs increases with timeToTrigger.

Effect of Changing hysteresis.

$$As \ \text{hysteresis} \Uparrow, \#HOs \Downarrow \ but \ \#RLFs \Uparrow . \quad (6)$$

Fig. 8 illustrates the effect of increasing hysteresis with the simple example of a single UE moving past two cells. As hysteresis increases, the UE requires a larger RSRP difference to trigger HO and can move away from a possible HO location without the completion of a successful HO, leading to lesser number of HOs. At the same time, as the UE moves away from the serving cell without completing a HO procedure, an RLF can be readily caused due to the degraded RSRP and thus SINR implying that the number of RLFs increases with hysteresis.

Effect of Changing a3offset.

$$As \ \text{a3offset} \Uparrow, \#HOs \Downarrow \ but \ \#RLFs \Uparrow . \quad (7)$$

Fig. 9 illustrates the effect of increasing a3offset with the simple example of a single UE moving past two cells. We observe from that a larger a3offset offsets the RSRP curve of the serving cell, for the purpose of the A3 algorithm, upwards, making it harder to trigger and perform a successful HO and easier to land into RLF due to the lack of HO. Hence, the a3offset parameter can be used to reduce unnecessary HOs.
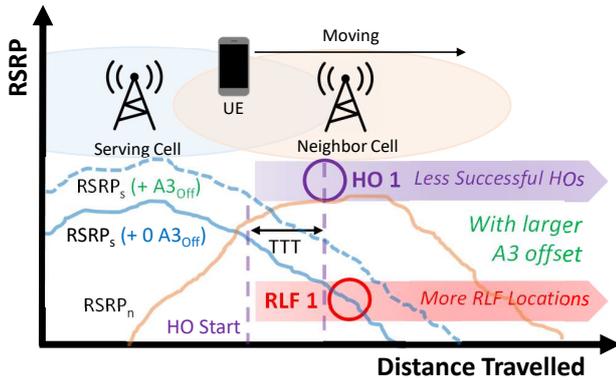
Figure 9. Effect of changing a3Offset on the number of HOs and RLFs; simple illustration with two cells and one UE

2.5. Relations About Combinations of HO Parameters

In this section, we discuss two relations involving combinations of HO parameters. The first relation in Section II.E.1 related to handover appears frequently in literature [4] [16] [3]. The second relation in Section II.E.1 is based on observing the effect of change in HO parameters (Section II.D.1 - II.D.4) on the observed number of HOs and RLFs. These provide good initial insight for extrapolation to HO performance in more complex scenarios involving more HO parameters.

Number of RLFs is proportional to `speed*timeToTrigger.`

$$\#\text{RLFs} \propto \texttt{speed} * \texttt{timeToTrigger} \tag{8}$$

This relation appears in several papers [4] [16] [3] as a result of model-based analysis, and indicates that the number of RLFs depends on the product of speed and `timeToTrigger`, rather than the individual quantities themselves. This relation is inituitive as number of RLFs increases with both speed and `timeToTrigger` as indicated by equation (4) and (5). Note that speed is a scenario parameter and `timeToTrigger` is an HO control parameter and this relation is about relationship between them and the number of RLFs. Hence, it gives a good idea on how the HO control parameters should be varied as per the scenario parameters to obtain the required results.

Inverse Relation Between Number of RLFs and HOs. The intuitive relations discussed in section II.D.3 to section II.D.5 point towards another intuitive relation. Note that when any of the HO control parameters is changed, the number of HOs and RLFs change in contrasting directions. This implies that over a large number of simulations or field trials, the number of HOs and RLFs

would be inversely proportional or rather follow an inverse trend.

2.6. Relations About Throughput

Network throughput is a complex quantity at the higher transport layer (layer 4) unlike the number of HOs and RLFs which are link layer (layer 2) quantities. Hence, the relation between HO control parameters of the link layer (layer 2) and the number of HOs & RLFs can be easily deduced as in the previous sections but not with the network throughput as it involves many more layers, quantities, and processes. Relations of the type described in the Section II.D and Section II.E cannot be arrived at for network throughput in terms of HO control parameters, making its prediction and optimization difficult. Hence, Gaussian process regression and bandit algorithms are proposed as good tools for the purpose of prediction and optimization of network throughput in Section 4.

However, the network throughput is expected to be impacted by increasing number of HOs and RLFs as they cause loss of connection. HOs cause only temporary interruption at the link layer, whereas RLFs cause complete loss of connection, changing the RRC state. Hence, the loss of throughput with RLFs is more profound than with HOs. This has been evidenced in Section IV.A with linear regression fits.

3. Simulation Results About HO Relations

The system setup for the simulations was discussed in detail in Section II. C and Table II. Initially, results from a *single* simulation run using our ns-3 code — the number of HO and RLFs - was collected. Thereafter, a larger number of parallel simulations with the ns-3 + SEM platform described in Section II.C was used for validation of the causal relations among input parameters and output, as discussed in Section II.D. Building upon this, the relations about combination of HO parameters in Section II.E are validated in Section III.C and new ones discovered in Section III.D. A short summary of the runtime details and the simulation hardware is presented at the end.

3.1. Sample Simulation Run

The source code is available here [27] along with the commands to configure and run a single simulation. The log messages obtained from a simulation are parsed in the python script to obtain the number of HOs and RLFs. When running a large number of simulations in parallel in SEM, the same parsing process is performed for each of the simulation runs and the compiled results stored in a file. The source code provides scripts to generate all the result figures in this paper.
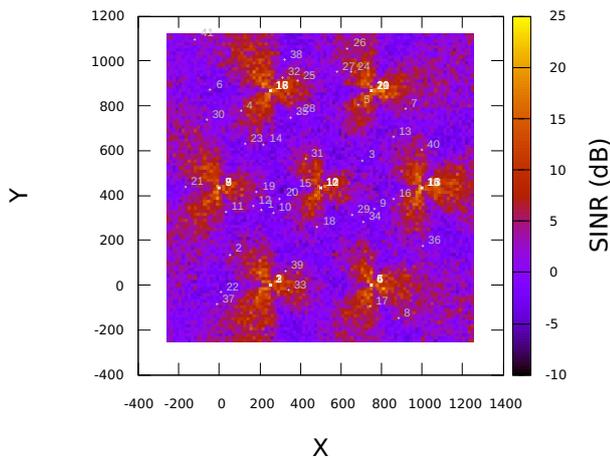
Figure 10. REM for sample simulation run of the `lena-dual-stripe` scenario

Table 3. Intercept (a), coefficient (b) and R^2 values obtained by linear regression for the relations validated in Fig. 11

Quantity	# HOs			# RLFs		
	a	b	R^2	a	b	R^2
speed	-1.9	0.42	0.52	2.53	5e-2	5e-2
timeToTrigger	42.5	-1e-2	0.25	2.39	5e-3	0.43
hysteresis	6.06	-0.49	0.52	1.82	0.11	0.39
a3Offset	23.7	-2.39	0.59	0.77	9e-2	0.33

Fig. 10 displays the radio environment map (REM) for the sample simulation run. As can be seen, this is a dense scenario with many UEs (≈50) and 21 closely spaced cells. Hence, by just running the simulation for a nominal 5s we can obtain statistically significant results for # of HOs and RLFs for a particular set of HO control parameters, as the UEs can traverse many cells in the duration of a simulaton run. Given that individual HO and RLF events occupy 40 ms and 100 ms respectively, using 5s = 5000 ms as the simulation run duration is a reasonable choice with ≈50 UEs moving and tens of HOs occurring. 5s gives a good number of HOs and RLFs with small variations accross simulations and a larger number for the simulation time would give similar but scaled numbers. In the next two subsections, simulation runs are performed with the standard values of the HO parameters in Table 1 to validate the relations in Section II.D and II.E. In all the graphs, each plotted point represents the result of one simulation run on this platform.

3.2. Validating Relations for Individual HO Parameters

Fig. 11 validates each of the relations for individual HO parameters claimed in Section 2.4 by plotting the

number of HOs and RLFs versus the various inputs individually, i.e., `speed`, `timeToTrigger`, `hysteresis` or `a3Offset` while keeping the others fixed. Each point on the lines (either blue or red) represents the result of the number of HOs (blue) or RLFs (red) from one simulation run. The first plot illustrates the impact of the speed parameter as discussed in Section II.D.1, by plotting the number of HOs and RLFs with (`a3Offset`, `timeToTrigger`, `hysteresis`) fixed at (0 dB, 1024 ms, 3 dB). As speed increases along the values- {10 m/s, 20 m/s ..., 120 ms/s}, we note that both the number of HOs and RLFs increase.

The values of intercept, coefficient and R^2 obtained by linear regression over a larger parameter set, are shown in Table 3. The R^2 values are < 0.6, implying that number of HO or RLFs are not purely linearly related to speed. However, for `timeToTrigger`, `hysteresis` and `a3Offset`, note that the coefficient (or slope) for # HOs and # RLFs show negative and positive correlation, respective. Yet, in the case of `speed`, these are both positive as discussed in Section II.D.1. The exact value of the coefficient and intercept in each of plots depends on the scenario parameters and HO control parameters that are not varied.

3.3. Validating Relations for Combinations of HO Parameters

To confirm the relation described in Section II.E.1, we perform simulations over the entire parameter set of the combination of `speed` = {10.0, 20.0, 30.0 ..., 160.0} and standard `timeToTrigger` values as per Table 1 resulting in 16 x 16 = 256 parameters. The result of each simulation run is plotted as a blue dot with the X-coordinate as the `speed*timeToTrigger` and the Y-coordinate as the number of RLFs in Fig. 12. The proportionality relationship between the number of RLFs and `speed*timeToTrigger` is validated by fitting a straight linear regression line (red) between the two quantities. The R^2 value of the fit is 0.6475 which implies that a large amount of the variance is explained and the model is worth attention. For reference, the intercept and coefficient obtained are -0.7050 and 0.0002 respectively.

To validate the inverse relation in Section II.E.2, a large number of simulations are performed with inputs of `timeToTrigger`, `hysteresis` and `a3Offset` sampled randomly from typical values of {0 ms, 40 ms, 64 ms, 100 ms, 128 ms, 160 ms, 256 ms, 320 ms, 480 ms}, {0 dB, 0.5 dB, ... 9.5 dB, 10dB} and {-3 dB, -2.5 dB ..., 0 dB, ... 2.5 dB, 3dB} respectively. Fig. 13 plots the results of the simulations as green density bubbles with the sizes as the frequency of that value and the X-coordinates and Y-coordinates representing the number of HOs and RLFs obtained as a result of the simulation runs. The
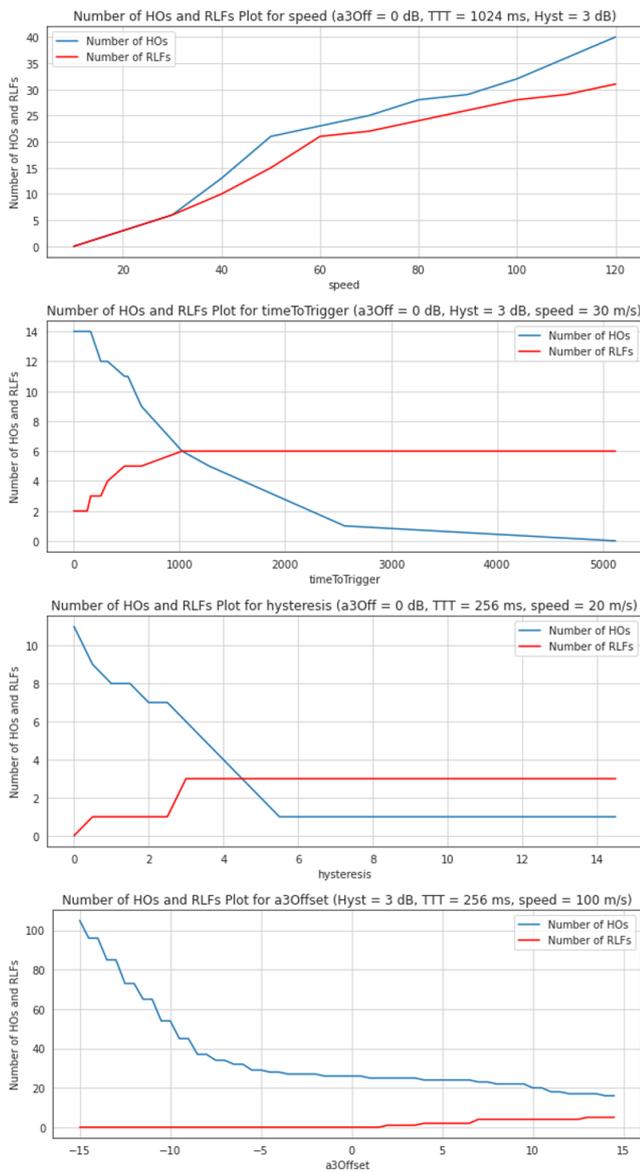
Figure 11. Validation of the individual relations for `speed`, `timeToTrigger`, `hysteresis` and `a3Offset` to the number of HOs and RLFs

Figure 12. Validation of the HO failure relation in literature– number of RLFs is proportional to `speed x timeToTrigger` (m/s * ms)

Figure 13. Investigation of the inverse relationship or trend between the number of HOs and RLFs

inverse relation between the number of HOs and RLFs is showcased by the red trend line. This implies that these are contradictory in nature and it is not possible to minimize both. Yet, both have an impact on the throughput and one wishes to simultaneously reduce both.

3.4. Discovering New Relations About HO Parameters

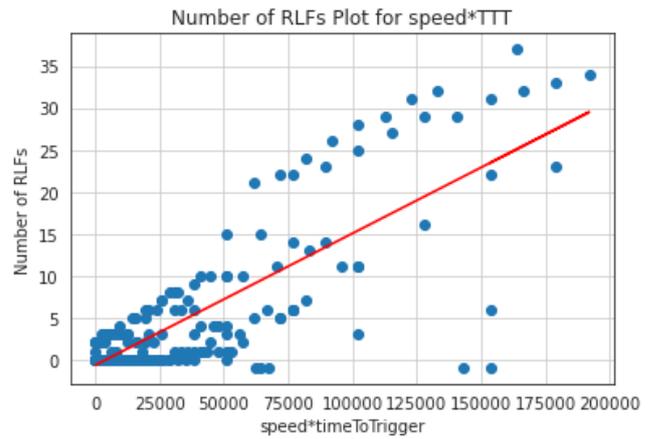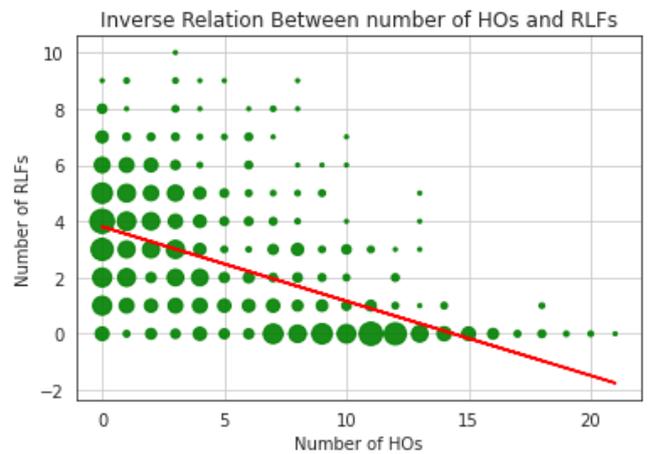In this subsection, we showcase the results obtained by running simulations using this platform for combinations of parameters that have not been studied well in the literature leading to the discovery of new relations from HO parameters to number of HOs and RLFs.

Fig. 14 illustrates the counterpart, for HOs, of Fig. 12 with the same simulation parameter set with 256 simulations. If only speed and `timeToTrigger` are varied, the number of handovers tends to be proportional to speed/`timeToTrigger` (red trend line). In other words, the number of HOs is dependent on the quantity speed/`timeToTrigger` rather than the individual quantities themselves as described in equation (9). The coefficient, intercept and R^2 values of the linear regression fit are 35.4779, 17.2003 and 0.4104. The low R^2 value indicates that there are several almost parallel trend lines indicating this
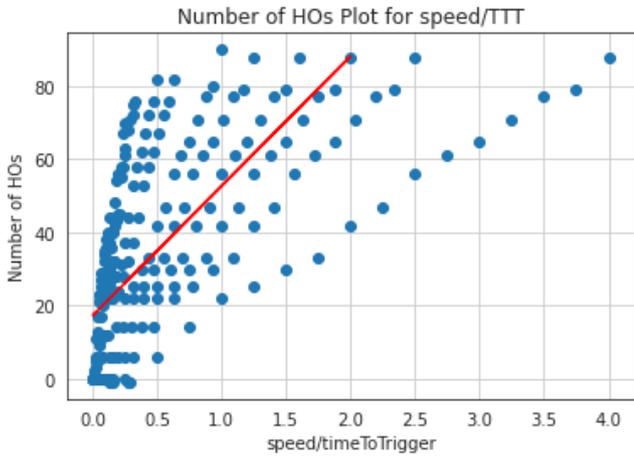
Figure 14. Investigation of a new relationship– number of HOs tends to be proportional to `speed/timeToTrigger` (m/s / ms)
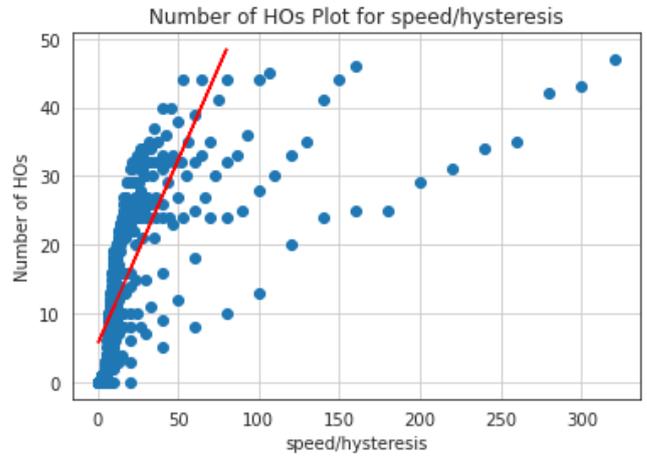

Figure 16. Investigation of a new relationship: number of HOs tends to be proportional to `speed/hysteresis` (dB/ (m/s))
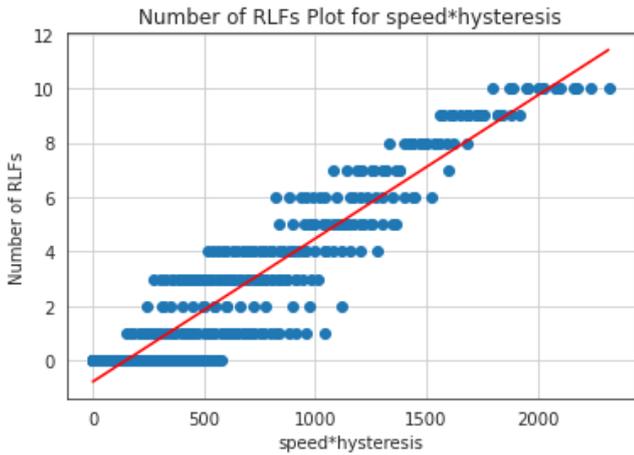

Figure 15. Investigation of a new relationship– number of RLFs is proportional to `speed*hysteresis` (dB m/s)

relation in Fig. 14. This is especially true at low values of `timeToTrigger` leading to higher values of `speed/timeToTrigger` in Fig. 14 and thus lower slopes.

$$\text{\#HOs} \propto \text{speed/timeToTrigger} \quad (9)$$

$$\text{\#RLFs} \propto \text{speed} * \text{hysteresis} \quad (10)$$

$$\text{\#HOs} \propto \text{speed/hysteresis} \quad (11)$$

Fig. 15 and Fig. 16 discuss new relationships related to the combination of `speed` and `hysteresis`. As described in relation (10) and (11), they take a similar form as their counterparts for the combination of `speed` and `timeToTrigger` in relation (8) and (9). From Fig. 15, we note that the number of RLFs or handover failures due to RLFs is directly proportional to `speed*hysteresis` as shown by the red regression

line. The coefficient, intercept and R^2 values of the linear regression fit in Fig. 15 are 0.0053, -0.7856 and 0.8834 respectively, with the high R^2 value indicating a strong fit with a large amount of variance explained. New relation (10) seems to hold over the entire parameter set. At the same time, we note from Fig. 16 that the number of HOs tends to be proportional to `speed/hysteresis`. The coefficient, intercept and R^2 values of the linear regression fit in Fig. 16 are 0.8061, 2.4111 and 0.6212 respectively. The high R^2 value indicates a strong fit but we notice some outlying points for which the relation seems to have a different lower slope in Fig. 16 for lower values of `hysteresis` and thus `speed/hysteresis`. Hence, we note that that the number of HOs and RLFs are dependent on these product and dividend expressions more than the individual quantities of `speed` and `hysteresis` themselves.

These relationships discovered through this simulation platform are entirely new and have not been discussed in the literature or investigated through simulation or field trials. These relations help mobile operators better understand the complementary nature of HOs and RLFs and the directions in which their numbers change when combinations of parameters are changed. Using them, they would be able to make the required adjustments to the HOs parameters in real-world networks to obtain gains of necessary quantities.

3.5. Runtime Details

The versions of ns-3 and SEM used to run the simulations were 3.35 and $0.3.1$ respectively. An nVIDIA GT75 Titan 8RG machine with 12 cores and 16 GB RAM was used to perform bulk of the simulations. Each simulation took about 30 seconds to run on an
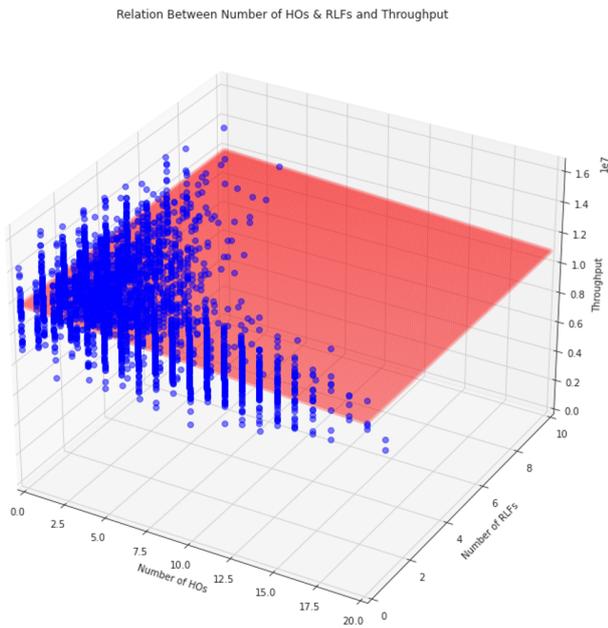
Figure 17. Throughput Variation with Number of HOs and RLFs

Figure 18. Gaussian Process Regression over `hysteresis` and `timeToTrigger` to predict network throughput

average allowing for a typical parameter set of 300–400 `parameters` to be explored in around 3 `hours`.

4. Throughput Analysis and Optimization

As explained in section 2.6, the relation between HO control parameters and throughput is not as simple as that for the number of HOs and RLFs. This section first demonstrates the impact of HOs and RLFs on network throughput through linear regression plots. The next subsection provides a good method for predicting the throughput at any given parameters using throughput output information obtained from a grid of input parameters using Gaussian process regression. Finally, throughput optimization over time with respect to HO control parameters is illustrated using bandit algorithms. In this paper, the throughput that is considered is the application layer throughput, i.e., the total number of bytes in received internet protocol packets divided by the total simulation time.

4.1. Throughput Variation with HOs and RLFs

Fig. 17 illustrates the throughput variation with the number of HOs and RLFs. The regression coefficients for the number of HOs and RLFs are 4818.8062 and -142990.8082 respectively. This indicates that there is a large decrease of throughput for every additional RLF as compared to HO. In the case of HO, there seems to be a negligible increase in throughput for every additional HO, but this is mainly due to the additional control
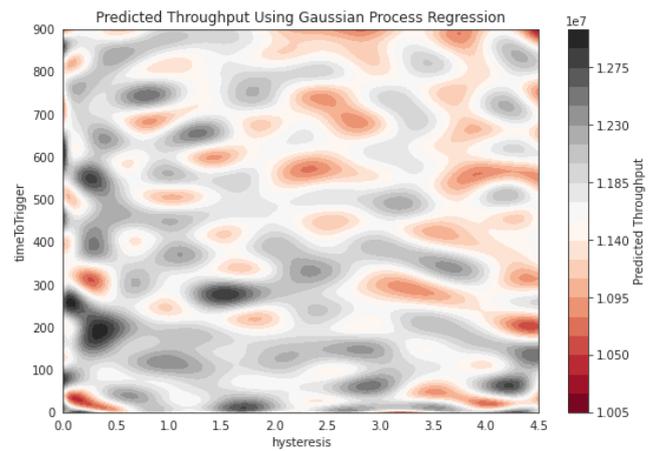
signals passed around due to the handover process and is not concerned with the data too much.

4.2. Throughput Prediction with Gaussian Process Regression

It is difficult to predict throughput at a given point in terms of the HO control parameters because network throughput is a transport layer quantity with complex relationship to `hysteresis`, `timeToTrigger` etc. This becomes especially important when a mobile network operator wants to carry out optimization over non-standard values in between the standard values specified in Table 1. We devise a novel method to predict the expected throughput at a given point by interpolation and estimation using Gaussian process regression from throughput values obtained from a grid of HO control parameters. We use gaussian process regression or Kriging as it gives the best linear unbiased prediction at unsampled locations and is known for its accuracy and adaptivity across the entire parameter set. A brief description of Gaussian process regression in relation to this problem is as below.

1. The function to be predicted, throughput in this case, is sampled at a number of pairs of the form (`hysteresis`, `timeToTrigger`), i.e., $\{(h_1, t_1), (h_2, t_2), ...(h_n, t_n)\}$.

2. A kernel function (say, radial basis function) $f(h, t | h_1, t_1, h_2, t_2 ... h_n, t_n) = g(h, t)$ is learned over the sampled points by optimizing its parameters based on them.

3. The prediction at a point (h', t') is given as $g(h', t')$. Hence, the function $g(h, t)$ learns to predict the throughput at any given point.

Our objective is to maximize the throughput under all `hysteresis` and `timeToTrigger` values as in (P1).

$$\begin{aligned} \underset{hyst, ttt}{\text{maximize}} \quad & Th(hyst, ttt) \\ \text{subject to} \quad & 0 \le hyst \le hyst_{max} \\ & 0 \le ttt \le ttt_{max} \end{aligned} \quad \text{(P1)}$$

where Th, hyst and ttt stand for throughput, `hysteresis` and `timeToTrigger` respectively.

Throughput values are obtained using ns-3 for each parameter set in the combination of `hysteresis` = {0 dB, 0.1 dB, 0.2 dB, ... 4.4 dB, 4.5dB} and `timeToTrigger` = {0 ms, 10 ms, ... 900 ms} with `speed` and `timeToTrigger` kept fixed at 30 m/s and 0 dB respectively. Gaussian process regression is used to learn a kernel function over this region and interpolate governed by prior covariances. The throughput values predicted at each point using the learned function are shown in Fig. 18 using the colour map. On performing optimization by sampling the throughput using this function over a 900 x 1800 grid, we get the maximum throughput as 1.3073e7 Kbps occuring at `hysteresis` & `timeToTrigger` of 100 ms & 3.83 dB respectively. The predicted value is within 1.4% of the actual value of 1.2886e7 Kbps obtained by performing an ns-3 simulation at this point.

4.3. Throughput Optimization Using Bandit Algorithms

This subsection considers the problem of throughput optimization over time. In real-world, this could take the form of throughput optimization by an operator for a given scenario over months or years by controlling the HO parameters appropriately. We note that the throughput values obtained for a given HO parameter set varies when the RngRun or RngSeed values are changed in the simulation platform due to presence of stochastic elements like fading and UE mobility. This represents the throughput values obtained for a given network by an operator over different time instants, whether hours, days or months.

Problem Formulation. Consider the problem of a mobile operator wanting to select the best `hysteresis` and `timeToTrigger` parameters for the problem of throughput optimization in a city over a long time period. At every time instant, the operate is presented with a row of 6 x 6 choices each representing a value in the parameter set of the combination of `hysteresis` = {0 dB, 1 dB, 3 dB, 5 dB, 7 dB, 9dB} and `timeToTrigger` = {0 ms, 100 ms, 256 ms, 480 ms, 1024 ms, 2560 ms}, assuming the other quantities are kept fixed. The multi-armed bandit can be seen as a set of real distributions of throughput over time $B = \{R_1, R_2, ... R_{36}\}$, each distribution R_i associated
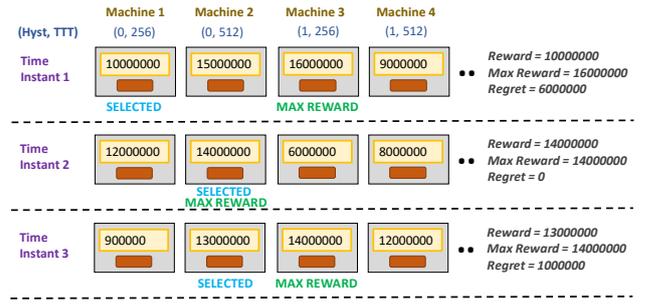

Figure 19. Throughput Optimization as an MAB Problem

with the throughput or reward obtained by selecting one of the 6 x 6 = 36 parameter sets available for `hysteresis` and `timeToTrigger` at every time instant. The operator selects one parameter set a out of the possible 36 at every time instant t and observes the associated throughput or reward- $r_{ta} = r_t$ sampled as per the distribution R_a. The regret x_t at a given instant t is the difference of the max possible reward at the given time and that of the chosen action as described by equation (12).

$$x_t = \hat{r}_t - r_t \text{ where } \hat{r}_t = \max_b r_{tb}, \ b \ \epsilon \{1, 2, ..., 36\} \quad (12)$$

The regret ρ_T after T time instants is the expected difference between the rewards associated with the optimal policy and the selected actions as described by equation (13).

$$\rho_T = \sum_{t=1}^{T} \hat{r}_t - \sum_{t=1}^{T} r_{ta} \quad (13)$$

The objective is to maximize the sum of rewards, i.e., minimize the total regret, over a long time horizon H. This is done through bandit algorithms to optimally select the actions at a given instant as per a policy. Average total regret is considered instead of total regret for purpose of understanding convergence over time periods. The reduction of average regret over time is a good indicator of a bandit algorithm's effectiveness.

Illustration. Fig. 19 shows an illustrative bandit algorithm for this problem, in which the parameter sets are selected at random at each time instant. At time instant 1, slot machine 1 or arm 1 representing `hysteresis` = 0 dB and `timeToTrigger` = 256 ms is selected giving a throughput or reward of, 10000000 Kbps. The maximum possible reward of, 16000000 Kbps is given by arm 3 at this time instant. The difference of the maximum possible reward and the obtained reward at a given time instant is called the regret and calculates to, 6000000 Kbps at this time instant. The regret at time

instant 2 is 0 Kbps, as the best parameter set is selected, and, 1000000 Kbps at time instant 3.

Solution. We implement the standard bandit algorithms for the problem of throughput optimization over time and plot the resultant average total reward for a time horizon of 1000 time instants as in Fig. 20. The three popular bandit algorithms of Explore-then-commit (ETC), ϵ-greedy and Upper Confidence Bound (UCB) were employed for this purpose. Initially, the algorithm or strategy needs to explore since it has less information about the rewards associated with each parameter set. But once the strategy gains enough information, it can exploit the parameter choices with high rewards or explore other parameter choices with less information. The aim of bandit algorithms is to strike an optimal balance between exploring all parameter choices so as to not miss out on valuable ones and exploiting the choices that have been the most profitable so far. The implementation details of the bandit algorithms used are given below.

1. ETC:
    This algorithm occurs in the below two stages and has a parameter num_exp.

    1. *Exploration-* Each of the parameter choices is made for num_exp respectively. The mean reward obtained for each parameter choice k is calculated as μ_k.

    2. *Exploitation-* The parameter set with the highest μ_k based on the exploration stage is selected for the rest of the time horizon.

2.ϵ-greedy: At a given time instant, the mean reward obtained until that instant for each parameter choice k is maintained as μ_k. A random number p is selected from $[0, 1]$ and one of the below steps is taken based on its value.

    1. $p < \epsilon$ *(exploration)-* a parameter choice is made uniformly at random

    2. $p \geq \epsilon$ *(exploitation)-* the parameter set with the highest μ_k is chosen

    The mean reward for the selected parameter set k- μ_k is updated after each step.

3.UCB: At a given time instant, the mean reward obtained until that instant for each parameter choice k is maintained as μ_k, the number of times that parameter is selected as n_k and the total number of steps taken as N. The UCB value of $\Delta_k = \mu_k + \sqrt{\frac{2logN}{n_k}}$ is calculated for each parameter set k. At each step the parameter set with the highest Δ_k is chosen and the UCB values updated. The UCB value and algorithm aims to strike a
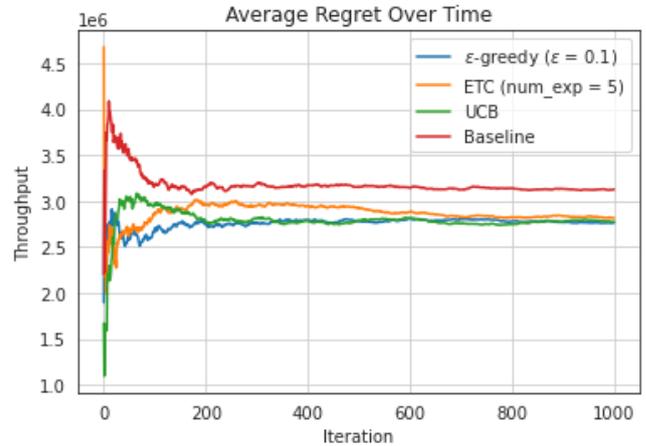

Figure 20. Average regret over time for various MAB algorithms

balance between the emprical mean reward μ_k and the exploration bonus of $\sqrt{\frac{2logN}{n_k}}$.

We note that the average regret for the three algorithms converges to around 2.80e7 Kbps for the parameter set in question as compared to the baseline of 3.12e7 Kbps obtained by selecting a fixed parameter configuration of (`hysteresis`, `timeToTrigger`) = (3 dB, 256 ms). Hence, bandit algorithms give statistically sound results for the problem of throughput optimization over time for LTE networks.

5. Conclusion

In this work, we explored various relations related to HO parameters by observing the A3 HO algorithm, in the context of enabling deeper understanding of HO modeling. Then we validated these relations pertaining to HO failures via ns-3 simulations, leveraging SEM capability for running a number of parallel simulations using multicore configuration composing a simulation platform in this process. Using the same platform, we discovered new HO relations never discussed in the literature. The validation of existing relations and discovery of new additional ones using this platform provides new insights to network operators to understand the impact of HOs and HO failures. Further exploiting this simulation platform, we shifted focus to the more complex quantity of throughput, quantifying its degradation, predicting resulting network throughput and devising algorithms for its optimization via choice of optimal HO control parameters. The algorithms devised for the choice of optimal parameters for network throughput in the presence of HO help them arrive at the best policies and parameters for network operations. This simulation platform boosts the credibility of the LENA module for use in HO modeling, analysis and algorithm discovery,

and will encourage further use among independent users and the industry.

Acknowledgments

References

[1] ANDREWS, J.G., BUZZI, S., CHOI, W., HANLY, S.V., LOZANO, A., SOONG, A.C.K. and ZHANG, J.C. (2014) What will 5g be? *IEEE Journal on Selected Areas in Communications* **32**(6): 1065–1082. doi:10.1109/JSAC.2014.2328098.

[2] DIMOU, K.D., WANG, M., YANG, Y., KAZMI, M., LARMO, A., PETTERSSON, J., MÜLLER, W. *et al.* (2009) Handover within 3gpp lte: Design principles and performance. *2009 IEEE 70th Vehicular Technology Conference Fall* : 1–5.

[3] NGUYEN, M.T. and KWON, S. (2020) Geometry-based analysis of optimal handover parameters for self-organizing networks. *IEEE Transactions on Wireless Communications* **PP**: 1–1. doi:10.1109/TWC.2020.2967668.

[4] CHEN, D., LIU, J., HUANG, Z., ZHANG, Z. and WU, J. (2015) Theoretical analysis of handover failure and no handover rates for heterogeneous networks. In *2015 International Conference on Wireless Communications Signal Processing (WCSP)*: 1–5. doi:10.1109/WCSP.2015.7341299.

[5] LEE, C., CHO, H.J., SONG, S. and CHUNG, J. (2020) Prediction-based conditional handover for 5g mm-wave networks: A deep-learning approach. *IEEE Vehicular Technology Magazine* **15**: 54–62.

[6] ERICSSON BLOG (2020), This is the key to mobility robustness in 5g netowrks. https://www.ericsson.com/en/blog/2020/5/the-key-to-mobility-robustness-5g-networks.

[7] PARK, H., LEE, Y., KIM, T., KIM, B.C. and LEE, J. (2021) Zeus: Handover algorithm for 5g to achieve zero handover failure. *ETRI Journal* doi:10.4218/etrij.2020-0356.

[8] JIANG, W. (2022) Graph-based deep learning for communication networks: A survey. *Computer Communications* **185**: 40–54. doi:https://doi.org/10.1016/j.comcom.2021.12.015, URL https://www.sciencedirect.com/science/article/pii/S0140366421004874.

[9] HE, S., XIONG, S., OU, Y., ZHANG, J., WANG, J., HUANG, Y. and ZHANG, Y. (2021) An overview on the application of graph neural networks in wireless networks. *IEEE Open Journal of the Communications Society* **PP**: 1–1. doi:10.1109/OJCOMS.2021.3128637.

[10] YANG, L., CHENG, M., QU, J. and CHEN, Z. (2022) Graphho: A graph-based handover optimization system for cellular networks. In *2022 International Symposium on Wireless Communication Systems (ISWCS)*: 1–6. doi:10.1109/ISWCS56560.2022.9940345.

[11] ZHAO, S., JIANG, X., JACOBSON, G., JANA, R., HSU, W.L., RUSTAMOV, R., TALASILA, M. *et al.* (2020) Cellular network traffic prediction incorporating handover: A graph convolutional approach. In *2020 17th Annual IEEE International Conference on Sensing, Communication, and Networking (SECON)*: 1–9. doi:10.1109/SECON48991.2020.9158437.

[12] BALDO, N., MIOZZO, M., REQUENA-ESTESO, M. and NIN-GUERRERO, J. (2011) An open source product-oriented lte network simulator based on ns-3. In *Proceedings of the 14th ACM International Conference on Modeling, Analysis and Simulation of Wireless and Mobile Systems*, MSWiM '11 (New York, NY, USA: Association for Computing Machinery): 293–298. doi:10.1145/2068897.2068948, URL https://doi.org/10.1145/2068897.2068948.

[13] BALDO, N., REQUENA-ESTESO, M., MIOZZO, M. and KWAN, R. (2013) An open source model for the simulation of lte handover scenarios and algorithms in ns-3. In *Proceedings of the 16th ACM International Conference on Modeling, Analysis &; Simulation of Wireless and Mobile Systems*, MSWiM '13 (New York, NY, USA: Association for Computing Machinery): 289–298. doi:10.1145/2507924.2507940, URL https://doi.org/10.1145/2507924.2507940.

[14] MAGRIN, D., ZHOU, D. and ZORZI, M. (2019) A simulation execution manager for ns-3: Encouraging reproducibility and simplifying statistical analysis of ns-3 simulations: 121–125. doi:10.1145/3345768.3355942.

[15] HERMAN, B., BALDO, N., MIOZZO, M., REQUENA, M. and FERRAGUT, J. (2014) Extensions to lte mobility functions for ns-3. In *Proceedings of the 2014 Workshop on Ns-3*, WNS3 '14 (New York, NY, USA: Association for Computing Machinery). doi:10.1145/2630777.2630779, URL https://doi.org/10.1145/2630777.2630779.

[16] LÓPEZ-PÉREZ, D., GUVENC, I. and CHU, X. (2012) Theoretical analysis of handover failure and ping-pong rates for heterogeneous networks. In *2012 IEEE International Conference on Communications (ICC)*: 6774–6779. doi:10.1109/ICC.2012.6364722.

[17] VASUDEVA, K., SIMSEK, M., LOPEZ-PEREZ, D. and GUVENC, I. (2015) Impact of channel fading on mobility management in heterogeneous networks. doi:10.1109/ICCW.2015.7247509.

[18] MARINESCU, A., MACALUSO, I. and DASILVA, L. (2017) System level evaluation and validation of the ns-3 lte module in 3gpp reference scenarios: 59–64. doi:10.1145/3132114.3132117.

[19] HENDRAWAN, H., ZAIN, A. and LESTARI, S. (2019) Performance evaluation of a2-a4-rsrq and a3-rsrp handover algorithms in lte network. *Jurnal Elektronika dan Telekomunikasi* **19**: 64. doi:10.14203/jet.v19.64-74.

[20] LIN, P.C., CASANOVA, L. and FATTY, B. (2016) Data-driven handover optimization in next generation mobile communication networks. *Mobile Information Systems* **2016**: 1–11. doi:10.1155/2016/2368427.

[21] LEE, Y., SHIN, B., LIM, J. and HONG, D. (2010) Effects of time-to-trigger parameter on handover performance in son-based lte systems. In *2010 16th Asia-Pacific Conference on Communications (APCC)*: 492–496. doi:10.1109/APCC.2010.5680001.

[22] Bae, H.D., Ryu, B. and Park, N.H. (2011) Analysis of handover failures in lte femtocell systems. In *2011 Australasian Telecommunication Networks and Applications Conference (ATNAC)*: 1–5. doi:10.1109/ATNAC.2011.6096636.

[23] Legg, P., Hui, G. and Johansson, J. (2010) A simulation study of lte intra-frequency handover performance. In *2010 IEEE 72nd Vehicular Technology Conference - Fall*: 1–5. doi:10.1109/VETECF.2010.5594477.

[24] (2020) *E-UTRA Radio Resource Control (RRC) protocol specification; Radio Resource Control (RRC); Protocol specification*. Tech. Rep. TS 36.331, 3GPP Release 16.

[25] (2020) *E-UTRA Radio Resource Control (RRC) protocol specification; Requirements for support of radio resource management*. Tech. Rep. TS 36.133, 3GPP Release 16.

[26] Alcatel-Lucent, p.D. and Vodafone (2009) *Simulation assumptions and parameters for FDD HeNB RF requirement*. Tech. Rep. R4-092042, 3GPP TSG RAN WG4.

[27] URL https://github.com/sachinnUW/ns-3-dev/tree/lena-sim.